J Appl Electrochem (2008) 38:1459–1466
DOI 10.1007/s10800-008-9590-7

ORIGINAL PAPER

Electrochemical formation and characterization of porous titania (TiO_2) films on Ti

Sahar A. Fadl-Allah · Rabab M. El-Sherief · Waheed A. Badawy

Received: 29 December 2007 / Accepted: 9 May 2008 / Published online: 31 May 2008

Abstract Galvanostatically and potentiostatically formed surface oxide films on titanium in H_2O_2 free and H_2O_2 containing H_2SO_4 solutions were investigated. Conventional electrochemical techniques, electrochemical impedance spectroscopy (EIS) and scanning electron microscopy, were used. In the absence of H_2O_2, the impedance response indicated a stable thin oxide film which depends on the mode of anodization of the metal. However, in the presence of H_2O_2 the film characteristics were changed. A significant decrease in the corrosion resistance of the surface film was recorded. The film characteristics were also found to be affected by the mode of oxide film growth and polarization time. The EIS results and the impedance data fitting to equivalent circuit models have shown that the oxide film consists of two layers. The electrochemical characteristics of the anodic films formed under different conditions have been discussed.

Keywords Anodic oxide films · Hydrogen peroxide · Impedance · Polarization · Passive films · Sulfuric acid

1 Introduction

Titanium and its alloys represent an important category of materials that have been used for many years in different industrial applications and as implant materials. This is partly due to the stable passive oxide films that could be formed on the material surface. In general, passive films compete with other techniques of surface protection, like phosphating, electro deposition of paints and others [1]. In high-tech systems, especially in micro and nanotechnology, passivation is competing with other micro structuring techniques, like PVD. The superior corrosion resistance of titanium and its alloys in comparison to stainless steels has been widely reported [2, 3]. Titanium oxide thin films with nanoporous structures are desirable due to their large surface area and high compatibility as clinical implant materials [4]. The good biocompatibility and osteointegrability of titanium are due to the presence of a very thin and adherent film, which is spontaneously formed on the metal surface. This so called passive condition of titanium, when placed in a physiological environment, gives good corrosion resistance. On the other hand, the presence of the oxide layer on the surface plays an important role in the favorable tissue response to titanium implants [4]. The biocompatibility is determined by the chemical processes occurring at the interface between prostheses and organic tissue which in the case of titanium, consists of a TiO_2 layer [4, 5]. It is possible to increase the range of biomaterial applications by depositing a thicker layer of TiO_2 on the metal surface [6] or by covering it with another biocompatible material, e.g., hydroxyapatite $Ca_{10}(PO_4)_6(OH)_2$ [7]. Titanium oxide surfaces show a wide range of structural and chemical properties, depending on their preparation and handling. The biocompatibility of titanium implants can be improved through oxide layer growth by several surface techniques like heat treatment, sol–gel preparations or anodic oxidation [8, 9]. The anodic oxidation of titanium alloys is a favorable procedure that has been proposed to improve the wear resistance and the adhesive properties of these materials [10]. The improvement has been extended to the biocompatibility of their surfaces [11, 12]. The biological performance of titanium oxide films was attributed to the morphology and structure

S. A. Fadl-Allah · R. M. El-Sherief · W. A. Badawy (✉)
Chemistry Department, Faculty of Science, University of Cairo, Gamaa Street, 12613 Giza, Egypt
e-mail: wbadawy@chem-sci.cu.edu.eg; wbadawy50@hotmail.com; wbadawy@wbadawy.csc.org.eg

of the films [13]. The approach of anodic oxidation to form porous titanium oxide films of controllable pore size, good uniformity and conformability over large areas at low cost constitutes a great challenge.

Various electrochemical techniques, including ac-impedance spectroscopy, photo-electrochemistry, scanning electron microscopy (SEM) and ellipsometric studies have demonstrated the changes in the growth rate and film properties with anodizing conditions [14–22]. During the last decades, anodic oxide films on titanium have been characterized by electrochemical impedance spectroscopy (EIS) [23–25].

The aim of this work was the optimization of the preparation conditions of porous TiO_2 films on Ti for biomedical applications. In this respect, Ti was anodized in H_2O_2 free and H_2O_2 containing H_2SO_4 solutions. The formed oxide films were investigated by conventional electrochemical techniques and EIS. A comparison was made between the oxide films formed galvanostatically and those formed potentiostatically under the same conditions. The porous films were examined by scanning electron microscope.

2 Experimental

The substrate material used was commercially pure Ti. The exposed circular surface area of the investigated material was 1.0 cm^2. Prior to immersion in the electrolyte, the electrodes were abraded using successive grades of emery paper down to 2,000 girt, then rubbed with a soft cloth until they acquired a mirror bright surface and washed with triple distilled water. The electrochemical set-up, electrochemical cell and methodology were as previously reported [26].

For oxide film preparation, two sets of experiments were performed in parallel. In One set, passive films on titanium were formed galvanostatically in H_2O_2 free and H_2O_2 containing 0.5 M H_2SO_4 at different current densities between 10 and 100 mA cm^{-2} for 30 min. In the second set of experiments, the passive films were formed potentiostatically at different anodization potentials between 1 and 10 V in the same electrolyte and also for 30 min. After anodization, the electrode impedance was followed as a function of time. In order to reduce phase shift errors at high frequencies a low impedance reference system was established connecting a platinum probe in parallel to the reference electrode by a 10-μF capacitance. The Haber-Luggin capillary of the reference electrode and the platinum probe were adjusted at nearly the same distance to the working electrode surface. All measurements were carried out in naturally aerated solutions at a constant room temperature of 303 ± 2 K. All potentials were measured against and referred to the $Hg/Hg_2SO_4/Na_2SO_4$ reference electrode ($E^{\circ}_{nhe} = 0.64$ V).

The EIS experiments were performed by the use of the IM6d.AMOS system (Zahner Elektrik GMBH & Co., Kronach, Germany). The input signal was usually 10 mV peak to peak in the frequency domain 0.1 to 1×10^5 Hz. Before each experiment, the working electrode was immersed in the test solution until a steady-state potential was reached and then the impedance data were recorded. The data were fitted to a theoretical data obtained according to an equivalent circuit model using a complex non-linear least squares circuit fitting software [27]. Scanning electron micrographs were obtained using a JEOL-840 Electron probe micro analyzer.

3 Results and discussion

3.1 Oxide film formation and characterization

The titanium electrodes were anodized galvanostatically or potentiostatically in naturally aerated H_2O_2 free 0.5 M H_2SO_4 solutions. Characterization of the formed oxide films under different conditions was carried out by EIS.

The Bode impedance plots of galvanostatically formed oxide films on Ti for 30 min in H_2O_2 free 0.5 M H_2SO_4 at different current densities recorded after 2 h immersion are presented in Fig. 1. The impedance spectra represent the typical behavior of passivated titanium [24, 28, 29]. For comparison, the impedance data of potentiostatically passivated Ti under the same conditions is presented in Fig. 2. The passive film acquires an interference color, starting from light gold, deep gold, light blue, dark blue to violet depending on the anodization potential, which is in good agreement with previously reported data [8].

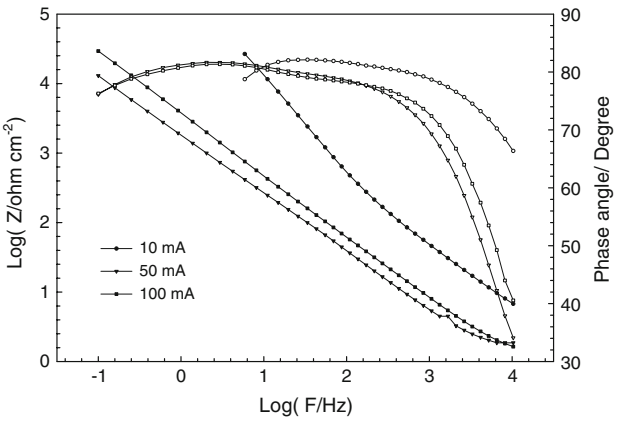

Fig. 1 Bode plots of oxide films formed galvanostatically for 30 min at different current densities in H_2O_2 free 0.5 M H_2SO_4 after 120 min of electrode immersion

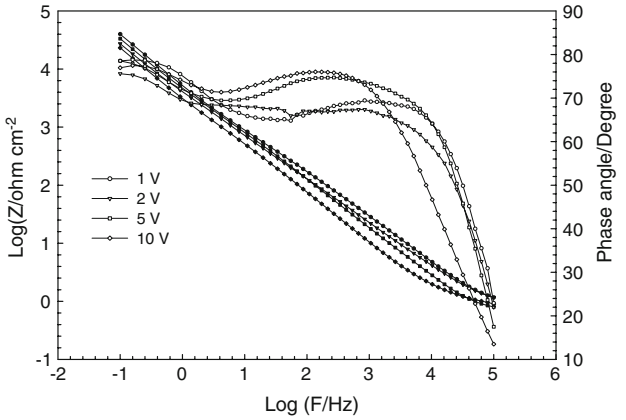

Fig. 2 Bode plots of oxide films formed potentiostatically for 30 min at different potentials in H_2O_2 free 0.5 M H_2SO_4 after 120 min of electrode immersion

The general features of the impedance plots are consistent with passive film behavior, which shows a phase angle approaching 90 °C over a wide frequency range [8, 24, 28–30].

As can be seen from the phase shift vs. log f presentation, in both Figs. 1 and 2, the electrochemical impedance responses display two time constants. This may be taken as evidence that the passive film formed on Ti, which was always described as a continuous single layer of TiO_2, is more likely to consist of two layers, a dense inner layer and a porous outer layer [31].

The experimental impedance data were fitted to theoretical data according to different equivalent circuits representing the electrode/electrolyte interface. The best fit

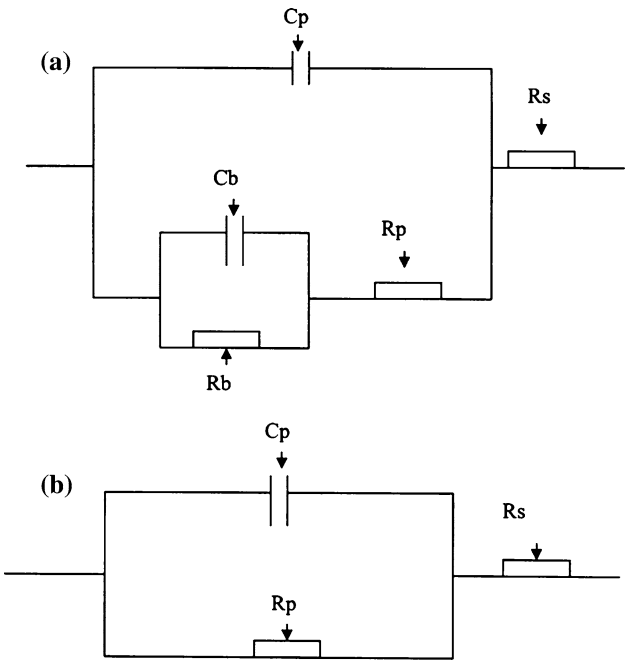

Fig. 3 Equivalent circuits models used for impedance data fitting of the oxide films formed on Ti under different formation conditions

was obtained using the equivalent circuit presented in Fig. 3a, where the duplex nature of the passive film was considered. In this model, the electrolyte resistance, R_s, is in series to two parallel combinations, R_b and C_b representing the barrier film resistance and capacitance, and R_p and C_p, representing the porous film resistance and capacitance, respectively. The results of data fitting according to this model for both the galvanostatically and potentiostatically formed oxide films are presented in Fig. 4a, b, respectively. There is excellent agreement between the experimental and theoretical data according to the proposed model. The slight deviation observed in Fig. 4a can be attributed to the fact that the oxide films formed galvanostatically are less homogeneous than those formed potentiostatically [32]. The values of the equivalent circuit parameters for the galvanostatically formed TiO_2 films at different current densities are presented in Table 1, and those of potentiostatically formed oxide at different potentials are presented in Table 2. It is clear that the values of the barrier film resistance, R_b, of films formed potentiostatically are relatively high and decrease with increase in anodization potential. For galvanostatically formed oxide films the value of C_b decreases and that of

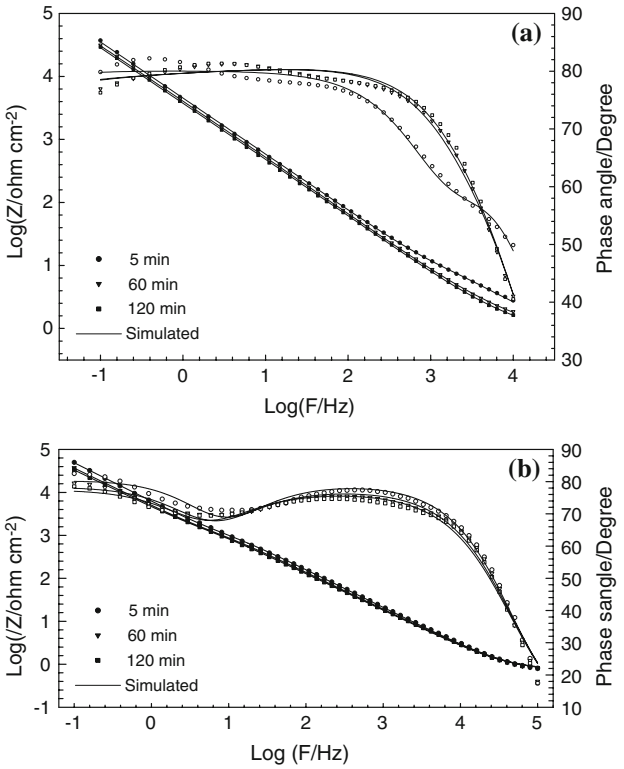

Fig. 4 (**a**) Bode plots of oxide films formed galvanostatically at 100 mA cm^{-2} in H_2O_2 free 0.5 M H_2SO_4 after different times of electrode immersion. Continuous lines represent simulated data. (**b**) Bode plots of oxide films formed potentiostatically at 5 V in H_2O_2 free 0.5 M H_2SO_4 after different times of electrode immersion. Continuous lines represent simulated data

Table 1 Equivalent circuit parameters for galvanostatically anodized Ti at different immersion times in H_2O_2 free 0.5 M H_2SO_4 at 25 °C

CD (mA cm^{-2})	Time (min)	R_p (kΩ cm^2)	R_b (MΩ cm^2)	C_p (μF cm^{-2})	C_b (μF cm^{-2})
10	5	0.5	3.9	6.4	0.76
	120	192.3	0.8×10^3	23.6	3.2×10^{-3}
50	5	1.1×10^3	5.5×10^3	14.8	0.012
	120	0.65×10^3	3.5×10^3	20.8	0.012
100	5	17.7×10^{-3}	6.7×10^3	9.6	6.8
	120	6.7×10^{-3}	3.2×10^3	15.2	5.6

Table 2 Equivalent circuit parameters for potentiostatically anodized Ti after 120 min of immersion in H_2O_2 free 0.5 M H_2SO_4 at 25 °C

Cell-voltage (V)	R_p (kΩ cm^2)	R_b (MΩ cm^2)	C_p (μF cm^{-2})	C_b (μF cm^{-2})
1	1.25	37×10^4	5.2	5.2
2	0.6	217×10^3	6.8	2.2
5	4.1	18.1×10^3	8.8	5.0
10	10.0	17.8×10^3	14.8	10.8

R_p increases with immersion time; this is attributable to slow oxide film growth that indicates long term stability of the oxide formed in H_2O_2 free H_2SO_4 solutions [23]. The increase in porous film capacitance, C_p, with increase in immersion time indicates porous film thinning. These results are in good agreement with the XPS investigations and independent optical measurements which suggest a small total thickness with a very thin outer porous layer [8].

The anodization technique affects both the mode of oxide film growth and the mechanism of film formation. Figure 5 shows a comparison between oxide films grown potentiostatically (Fig. 5a) and those formed galvanostatically (Fig. 5b). In both cases, a capacitive behavior of the passive film over a wide frequency range is recorded. For the films grown galvanostatically a single time constant controls the film formation kinetics, which implies that the compact inner layer is dominating. On the other hand, the films formed potentiostatically show a splitting in the log f vs. phase diagram (Fig. 5a) which means that the kinetics of film growth are controlled by two time constants, i.e., both the inner compact layer and the outer porous layer are contributing to the film growth kinetics.

3.2 Effect of H_2O_2 on passive film characterization

In this series of experiments the films were formed under the same conditions described in Sect. 3.1 in the presence of different concentrations of H_2O_2 in the anodizing solution. The impedance spectra of films formed galvanostatically at 100 mA cm^{-2} are presented in Fig. 6 and those of films formed potentiostatically at 5 V are presented in Fig. 7. Comparison between the data presented in Figs. 6 and 7 and those presented in Figs. 1 and 2 indicates that the presence of H_2O_2 changes the passive film properties. At low H_2O_2 concentration (≤0.1 M) two phase maxima in the impedance spectra were recorded. The impedance data of these measurements were also fitted to the equivalent circuit model presented in Fig. 3a. The data fitting indicates that the passive film consists of a dense inner layer of high

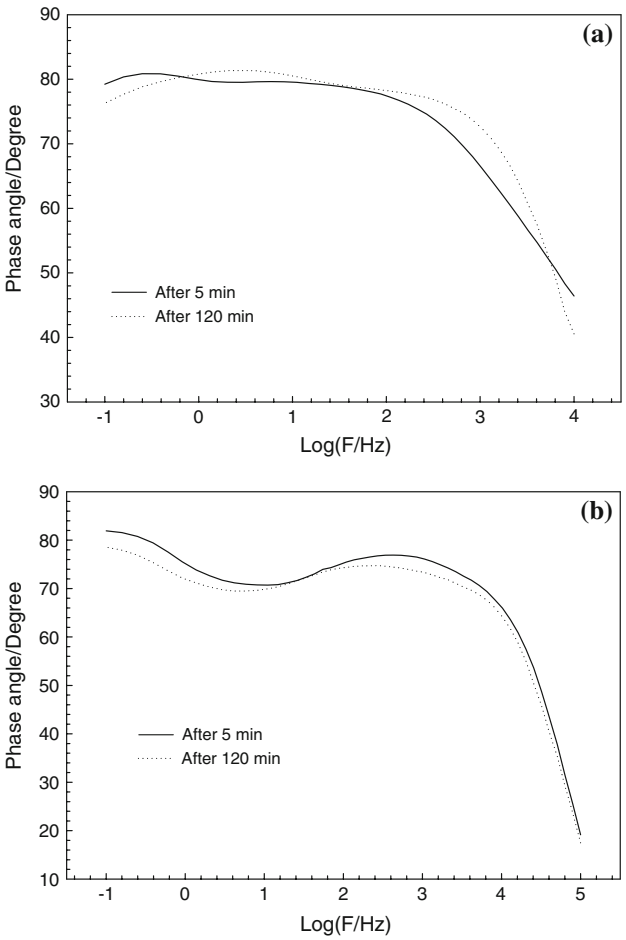

Fig. 5 Electrochemical impedance response of oxide film formed for 30 min (**a**) potentiostatically at 5 V, (**b**) galvanostatically at 100 mA cm^{-2} on Ti in H_2O_2 free 0.5 M H_2SO_4 after (1) 5 min and (2) 120 min time of electrode immersion

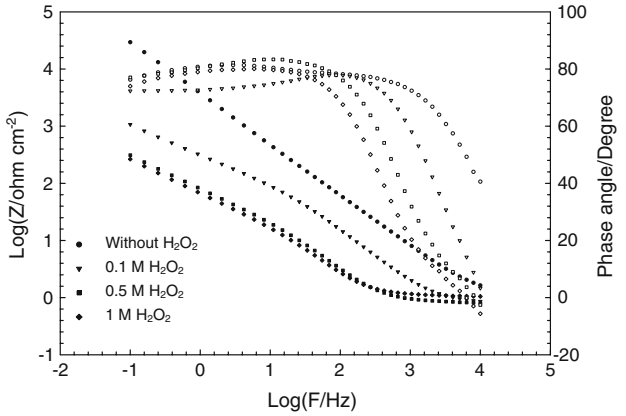

Fig. 6 Bode plots of oxide films formed galvanostatically at 100 mA cm^{-2} for 30 min on Ti in 0.5 M H_2SO_4 containing different concentrations of H_2O_2 after 120 min electrode immersion

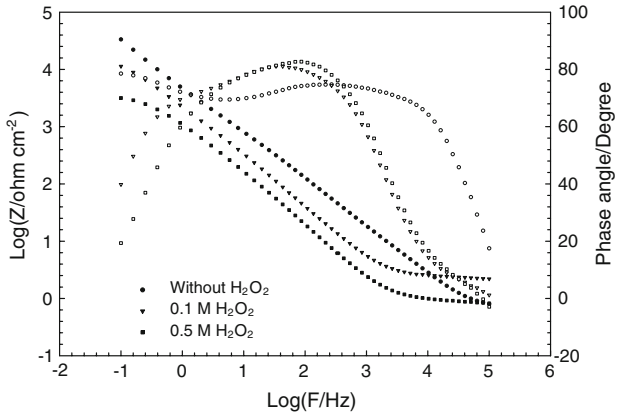

Fig. 7 Bode plots of oxide films formed potentiostatically at 5 V for 30 min on Ti in 0.5 M H_2SO_4 containing different concentrations of H_2O_2 after 120 min electrode immersion

corrosion resistance and an outer porous layer of relatively low resistance. The whole film thickness is small as inferred from the values of the capacitance.

At higher H_2O_2 concentrations (>0.5 M) in the anodizing solution a single phase maximum was recorded. This is characteristic for corroding systems governed by the simple Randles equivalent circuit presented in Fig. 3b [24, 30]. In this model R_p represents the charge transfer (corrosion) resistance of the passive film, C_p its capacitance and R_s is the ohmic drop in the electrolyte [23, 26].

The results of impedance data fitting are presented in Table 3. These results reveal that the increase in H_2O_2 concentration in the formation medium above 0.5 M leads to a decrease in barrier film resistance R_b, which means that the barrier film becomes defective and starts to dissolve. The presence of H_2O_2 leads to an increased rate of dissolution and the oxide film becomes thinner as reflected from the increased C_b values. It should be mentioned that the effect of H_2O_2 is the same, whether the oxidation process is carried out galvanostatically or potentiostatically (cf. Figs. 6, 7). The reason could be the partial reduction of the oxide by H_2O_2.

The effect of electrode immersion time before the impedance measurements on the equivalent circuit parameters is presented in Fig. 8a, b. The figure shows also the effect of the presence of H_2O_2. It is clear that the film formed in H_2O_2 free 0.5 M H_2SO_4 always has constant R_p and C_b values. Increase in H_2O_2 concentration above 0.5 M leads to passivity breakdown due to an immediate increase in the local conductivity [24, 33]. The passivity breakdown depends mainly on the electrolyte composition, its concentration, and to less extent on the current density, temperature and roughness factors [33].

To emphasize the effect of anodization potential in the potentiostatic formation mode, some oxide films were formed in H_2O_2 free H_2SO_4 solutions at 10 V under the same conditions. The impedance data were fitted to the theoretical models presented in Fig. 3. The results of these measurements are presented in Fig. 9. The addition of a small concentration of H_2O_2 leads to the disappearance of one of the two phase maxima, and only a single phase maximum is recorded. Deviation from the data fitting of oxide films formed at 5 V, especially in the presence of H_2O_2 can be observed. The deviation of the fitted experimental impedance values obtained with the passive films formed at 10 V compared to those films formed at 5 V leads to the conclusion that increase in formation voltage produces less homogeneous films of more defective nature [24, 32].

3.3 Film morphology

To obtain insight into the morphology of the surface film and the structural changes and also the effect of the presence of H_2O_2 in the electrolyte, the electrode surface was investigated by SEM as shown in Figs. 10 and 11.

The SE micrograph of the mechanically polished Ti surface represents the typical morphology of mechanically polished polycrystalline metallic surface (not shown). Figure 10 shows the micrographs of the potentiostatically anodized surface at 5 V in 0.5 M H_2SO_4 after immersion in H_2O_2 free 0.5 M H_2SO_4 for 30 min (Fig. 10a), after immersion in 0.1 M H_2O_2 containing 0.5 M H_2SO_4 for the same time (Fig. 10b) and after 30 min immersion in 1.0 M H_2O_2 containing 0.5 M H_2SO_4 solution (Fig. 10c). The surface treated in H_2O_2 free H_2SO_4 solutions is covered with a thin homogeneous compact film of uneven nanocrystals of TiO_2 [34]. The presence of such a homogeneous film is also confirmed by the electrochemical characteristics presented in Fig. 4.

Table 3 Equivalent circuit parameters for galvanostatically anodized Ti at 100 mA cm^{-2} after different immersion times in 0.5 M H_2SO_4 containing different H_2O_2 concentrations at 25 °C

$[H_2O_2]$ (M)	Time (min)	R_p (kΩ cm^2)	R_b (MΩ cm^2)	C_p (μF cm^{-2})	C_b (μF cm^{-2})
0	5	17.7×10^{-3}	6.7×10^3	9.6	6.8
	15	12.8×10^{-3}	7.0×10^3	10.8	6.4
	60	8×10^{-3}	4.8×10^3	14.0	6.0
	120	6.7×10^{-3}	3.2×10^3	15.2	5.6
0.1	5	1.55	20.5×10^3	5.8	5.2
	15	1.15	25.0×10^3	6.8	4.4
	60	0.43	18.8×10^3	8.8	3.5
	120	0.28	14.6×10^3	10.4	3.3
0.5	5	1.7×10^{-3}	68×10^3	5.6	12.8
	15	1.2×10^{-3}	0.5×10^3	8.8	12.0
	60	2.7×10^{-3}	90×10^3	17.6	9.6
	120	2.2×10^{-3}	29.3	24.8	10.0
1	5	1.5	29.7	20.0	4.8
	15	0.25	9.6	27.6	4.8
	60	3.7	–	42.6	–
	120	2.9	–	54.0	–

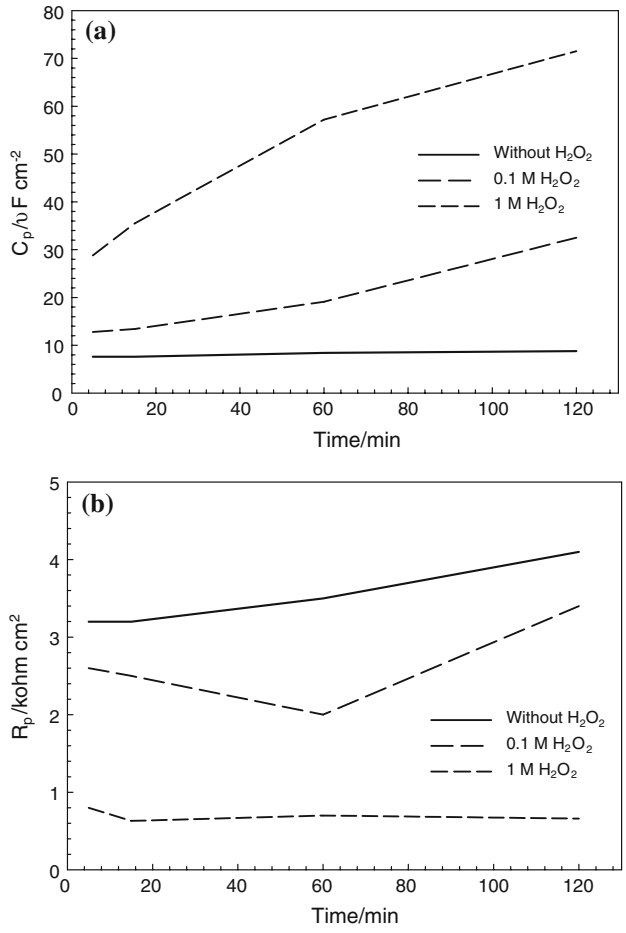

Fig. 8 Equivalent circuit parameters (**a**) Capacitance, C_p, and (**b**) Resistance, R_p, of the porous layer on Ti after different times of electrode immersion in: (1) H_2O_2 free 0.5 M H_2SO_4, (2) 0.5 M H_2SO_4 + 0.1 M H_2O_2 and (3) 0.5 M H_2SO_4 + 0.5 M H_2O_2

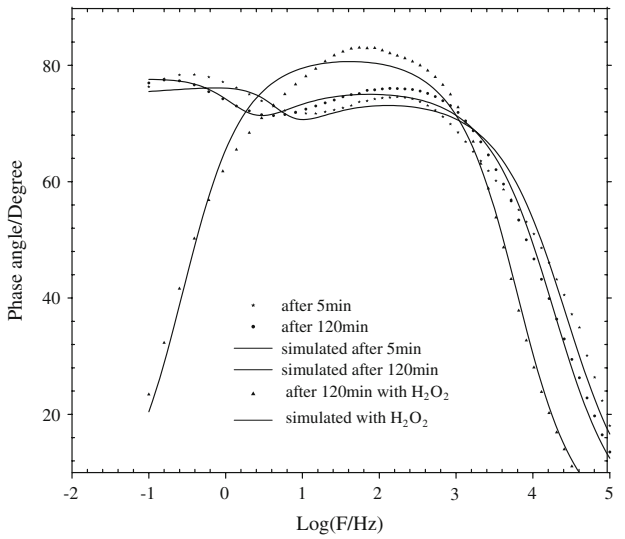

Fig. 9 Electrochemical impedance response of oxide film formed potentiostatically at 10 V on Ti in H_2SO_4 after (1) 5 min without H_2O_2, (2) 120 min without H_2O_2 and (3) 120 min in presence of 0.1 M H_2O_2

The presence of low concentrations of H_2O_2 (≤0.1 M) leads to the formation of dissolution patterns in the nano range which gives the nanoporous structure assigned to the outer layer (cf. Fig. 10b). Increase in the concentration of H_2O_2 (>0.5 M) leads to a continuous dissolution of the passive film and damage to the compact film is recorded (cf. Fig. 10c). Damage to this passive film is reflected in the passivity breakdown observed electrochemically [32].

The inhomogeneity assigned to passive films formed at 10 V was also confirmed by SEM. Figure 11 shows the micrograph of the film formed at 10 V after 30 min

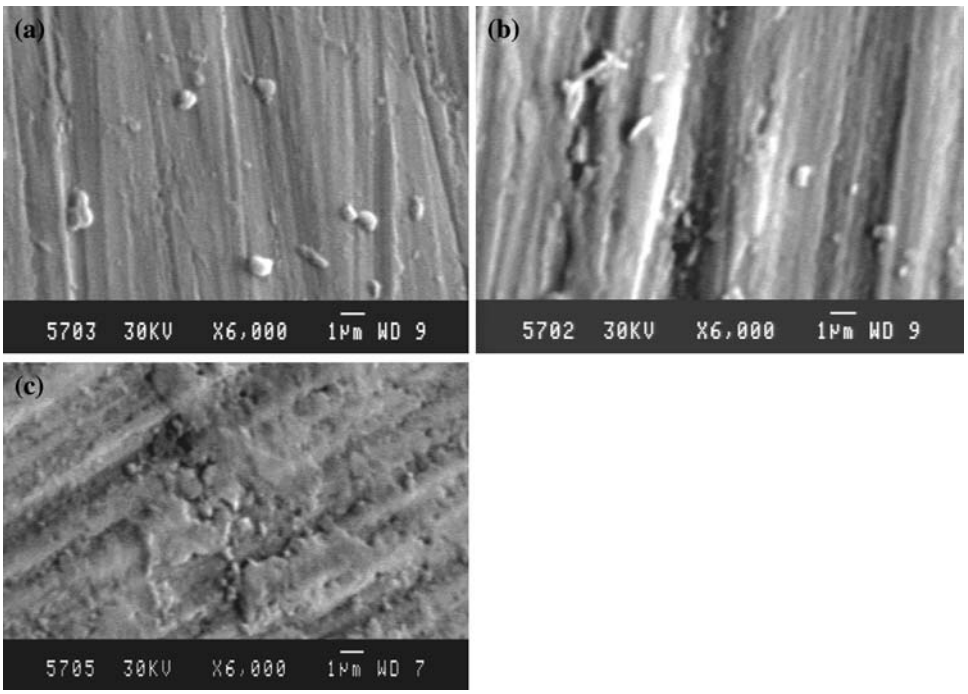

Fig. 10 Scanning electron micrographs of potentiostatically anodized Ti at 5 V for 30 min in (**a**) H_2O_2 free 0.5 M H_2SO_4, (**b**) 0.5 M H_2SO_4 + 0.1 M H_2O_2 and (**c**) 0.5 M H_2SO_4 + 1 M H_2O_2

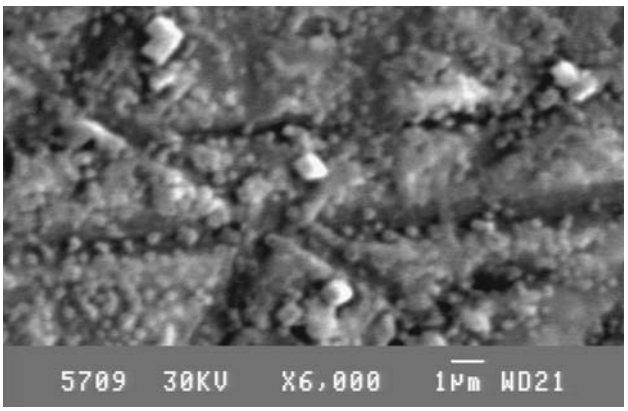

Fig. 11 Scanning electron micrograph of potentiostatically anodized Ti at 10 V in H_2O_2 free 0.5 M H_2SO_4 for 30 min

immersion in 0.5 M H_2SO_4. Comparison of this micrograph with that of the film formed at 5 V under the same conditions (Fig. 11a) clearly shows that the use of a higher formation voltage leads to heterogeneous passive films with microstructures as an outer layer which covers a dense compact film. The SEM results confirm the conclusions made from the experimental results of EIS.

4 Conclusions

The anodic oxide films formed on Ti surfaces in sulfuric acid solutions consist of two layers, an inner compact and an outer porous layer. The oxide film growth kinetics of the galvanostatically formed films are controlled by the compact layer, whereas those formed potentiostatically are controlled by both layers. The anodic oxide films formed galvanostatically at any current density or potentiostatically at higher voltages ($\geq$10 V) are less homogeneous and with more defective nature. Low concentrations of H_2O_2 ($\leq$0.1 M) in the anodizing solution lead to the formation of oxide films with nanoporous structure. The increase in H_2O_2 concentration leads to oxide film dissolution and passivity breakdown.

References

1. Schulze JW, Lohrengel MM (2000) Electrochim Acta 45:2499
2. Solar RJ (1979) In: Syrett A, Acharya A (eds) First international symposium on corrosion and degradation of implant materials. American Society for Testing and Materials, Philadelphia, p 259
3. Williams DF (1981) In: Williams DF (ed) Biocompatibility of clinical implant materials. CRC, Boca Raton, p 99
4. Ratner BD (1993) J Biomed Mater Res 27:837
5. Vogler EA (1996) J Electron Spectrosc Relat Phenom 81:237
6. Lausmaa J (1996) J Electron Spectrosc Relat Phenom 81:343
7. Montenero A, Ferrari F, Cesori M, Gnappi G, Salvioli E, Mattogno L, Kaciulis S (2000) J Mater Sci 35:1
8. Velten D, Biehl V, Aubertinetal F (2002) J Biomed Mater Res 59:18
9. Xiong TY, Cui XY, Kimetal HM (2004) Key Eng Mater 254:375
10. Sibert ME (1983) J Electrochem Soc 25:65
11. Kokubo T (1998) Acta Mater 46:2519
12. Sul YT (2003) Biomaterials 23:3893

13. Sul YT, Johansson CB, Jeong Y (2002) Clin Oral Implants Res 13:252
14. Blackwood DJ, Greef R, Peter LM (1989) Electrochim Acta 34:120
15. Blackwood DJ, Peter LM (1989) Electrochim Acta 34:1505
16. Kozlowski M, Smyrl WH, Atanasoska L, Atanasoski R (1989) Electrochim Acta 34:1763
17. Di Quarto F, Pizza S, Sunseri C (1993) Electrochim Acta 38:29
18. da Fonseca C, Ferreira MG, da Cunha Belo M (1994) Electrochim Acta 39:2197
19. Ohtsuka T, Nomura N (1997) Corros Sci 39:1253
20. Marsh J, Gorse D (1998) Electrochim Acta 43:659
21. Ohtsuka T, Otsuki T (1998) Corros Sci 40:951
22. Azumi K, Seo M (2001) Corros Sci 43:533
23. Cheng TP, Lee JT, Tsai WT (1991) Electrochim Acta 36:2069
24. Badawy WA, Elegamy SS, Ismail KhM (1993) Br Corros J 28:133
25. Kolman DG, Scully JR (1994) J Electrochem Soc 141:2633
26. Badawy WA, Al-Kharafi FM, El-Azab AS (1999) Corros Sci 41:709
27. Macdonald JR (2005) Solid State Ionics 176:1961
28. Felske A, Badawy WA, Plieth WJ (1990) J Electrochem Soc 137:1804
29. Badawy WA, Ismail KhM (1993) Electrochim Acta 38:233
30. Garcia I, De Damborenea JJ (1998) Corros Sci 40:1411
31. Tomashov ND, Chernova GP, Ruscol YuS, Ayuyan GA (1974) Electrochim Acta 19:159
32. Pan J, Thierry D, Leygraf C (1996) Electrochim Acta 41:1143
33. Sato N, Okamoto G (1981) In: Bockris JOM (ed) Comprehensive treatise of electrochemistry, vol 4. p 193, Plenum Press, New York
34. Katerini A, Mantzila G, Prodromidis MI (2006) Electrochim Acta 51:3537